50 YEARS
eISSN 1981-1829
Ciência e Agrotecnologia
Science and Agrotechnology

# Mathematical modeling of passion fruit peel and flour quality after drying

## Modelagem matemática da casca de maracujá e qualidade da farinha após a secagem

Geraldo Acácio Mabasso[1*], Adrielle Borges de Almeida[2], Samuel Ferreira Viana[2], Juliana Aparecida Célia[2], Osvaldo Resende[2], Daniel Emanuel Cabral de Oliveira[2]

### ABSTRACT

Passion fruit peel can be used as an alternative for nutrients available in the fruit peel, which is normally discarded during pulping. Therefore, in this study, we analyzed the drying kinetics of passion fruit peel and evaluated the effect of drying temperature on the physicochemical and technological characteristics of the flour derived from the product obtained at different temperatures (50, 60, and 70 °C). The experimental drying data were adjusted to mathematical models based on nonlinear regression analysis using the Gauss-Newton method and supplemented by the Akaike Information Criterion (AIC) and Bayesian Information Criterion (BIC). The physicochemical, technological, and color characteristics were evaluated using a completely randomized design, with three temperatures and five repetitions. The Valcam model presented the best fit at 50 and 70 °C, and the Page model presented the best fit at 60 °C. The effective diffusion coefficient ranged from $6.87 \times 10^{-10}$ to $15.04 \times 10^{-10}$ $m^2\ s^{-1}$ for temperatures of 50–70 °C, and the activation energy was 36.144 kJ $mol^{-1}$. For the flour, the increase in drying air temperature negatively affected quality parameters, except for water absorption capacity, water solubility, and ash content, with a temperature of 50 °C being the best suited to maintaining the quality of passion fruit peel flour.

**Index terms**: Scanning electron microscopy; physicochemical characteristics; *Passiflora edulis* Sims; drying kinetics.

### RESUMO

A casca do maracujá é uma alternativa para o aproveitamento dos nutrientes disponíveis na casca do fruto que normalmente é descartada no momento da despolpa. Sendo assim objetivou-se com esse trabalho analisar a cinética de secagem da casca de maracujá, bem como avaliar a influência da temperatura de secagem nas características físico-químicas e tecnológicas da farinha do produto obtida nas temperaturas 50, 60 e 70 ºC. Aos dados experimentais de secagem foram ajustados os modelos matemáticos, a partir de análise de regressão não-linear pelo método Gauss Newton e complementados pelo Critério de Informação de Akaike (AIC) e Critério de Informação Bayesiano (BIC). Os dados sobre as características físico-químicas, tecnológicas e cor, foram avaliados em Delineamento Inteiramente Casualizado, considerando as três temperaturas e cinco repetições. Conclui-se que o modelo de Valcam apresentou melhor ajuste nas temperaturas de 50 e 70 ºC e o de Page para temperatura de 60 ºC; o coeficiente de difusão efetivo variou de $6,87 \times 10^{-10}$ à $15,04 \times 10^{-10}$ $m^2\ s^{-1}$ para a faixa de temperatura de 50 à 70 ºC e a energia de ativação foi de 36,144 kJ $mol^{-1}$. Para a farinha o aumento da temperatura do ar de secagem influenciou negativamente nos parâmetros de qualidade, com exceção da capacidade de absorção em água, solubilidade em água e teor de cinzas, sendo a temperatura de 50 ºC a que melhor manteve a qualidade da farinha de casca de maracujá.

**Termos para indexação**: Microscopia eletrônica de varredura; características físico-químicas; *Passiflora edulis* Sims; cinética de secagem.

Food Science and Technology

Ciênc. Agrotec., 50:e024425, 2026
http://dx.doi.org/10.1590/1413-7054202650024425

Editor: Renato Paiva

[1]Universidade Zambeze/UniZambeze, Faculdade de Engenharia Ambiental e dos Recursos Naturais/FEARN, Chimoio, Manica, Moçambique
[2]Instituto Federal de Educação, Ciência e Tecnologia Goiano/IF Goiano, Laboratório de Pós-Colheita de Produtos Vegetais/LPCPV, Rio Verde, Go, Brasil

*Corresponding author: geral.do@hotmail.com

*Received in December 10, 2025 and approved in May 7, 2026*

## Introduction

Brazil accounts for approximately 65% of global passion fruit production, followed by Colombia and Indonesia. The passion fruit species *Passiflora edulis* Sims (yellow passion fruit or sour passion fruit) has very high commercial demand (Junghans, 2022). Recently, the global demand for passion fruit and its derivatives has increased considerably due to their nutritional and functional properties, particularly in tropical and subtropical regions (Fonseca, Silvestre & Rocha, 2025; Infante-Neta et al., 2026).

The peel (epicarp) of passion fruit is discarded in the juice and pulp industries; it may have characteristics of technological (proximate compositions, insoluble and soluble fiber contents) and biological interest (Martínez et al., 2012). Juice production generates large amounts of agro-industrial waste in the form of peels and seeds. This waste represents 76% of the raw material mass after fruit processing (Leão et al., 2014). Up to 60–70% of the fruit mass is discarded during processing, which significantly increases environmental burden while simultaneously representing a valuable source of bioactive compounds such as dietary fiber, pectin, and phenolic compounds (Betancur-Ancona et al., 2025; Teles et al., 2023).

Maximizing the value of byproducts from fruit processing for juice production is essential from an environmental, economic, scientific, and technological perspective. Santos et al. (2021) found that the food production industry generates a large amount of byproducts that can be reused, such as passion fruit pulp, peel, and seeds. Studies characterizing food industry byproducts can contribute to their valorization (Nguyen et al., 2019; Infante-Neta et al., 2026). Within the framework of a circular bioeconomy, the valorization of agro-industrial residues has received much attention, with applications ranging from food ingredients to biomaterials and biopolymers, reinforcing the need for efficient processing strategies (Infante-Neta et al., 2026).

Some studies have reported that plant-based materials and agro-industrial residues can be incorporated into bakery products. Biscuits fortified with *Moringa oleifera* and *Camellia sinensis* showed greater nutritional value and consumer acceptance (Moin et al., 2024). Similarly, adding Kinnow (*Citrus reticulata*) peel to bread increased the content of dietary fiber and modified physicochemical and sensory properties (Kaur et al., 2023). These findings indicate that fruit peels can serve as sustainable raw materials, thereby encouraging further investigation of passion fruit peel as a source of flour.

Drying is an important method for processing and preserving plant products, such as passion fruit peel. However, the main criteria must be established to ensure that the process does not affect the final quality, for example, the air temperature used for drying (Nascimento et al., 2016). Drying is a complex heat and mass transfer process influenced by temperature, air velocity, and the structure of the material; it affects the physicochemical properties and the retention of bioactive compounds (Cavalcanti-Mata et al., 2024). Functional and bioactive properties need to be maintained while drying for their use as food ingredients. Owing to their high content of dietary fiber and phenolic compounds, passion fruit peel exhibits antioxidant potential; however, these compounds are sensitive to processing conditions, particularly temperature (Gunjal et al., 2025).

Drying preserves the quality of most agricultural products. When performed correctly, it preserves the product, protects against enzymatic degradation and oxidation, and contributes to more suitable storage conditions (Quequeto et al., 2019; Siqueira et al., 2020), as each product has specific characteristics associated with drying. Optimal drying conditions decrease energy consumption while preserving product quality (Sittipa et al., 2020). Drying efficiency and its effect on quality depend on temperature, influencing the removal of moisture, retention of bioactive compounds, and structural stability (Demircan, Velioglu, & Giuffrè, 2023; Sousa et al., 2024). Thus, temperature optimization must consider the characteristics of raw materials and their intended use.

Mathematical modeling of drying kinetics is widely performed to predict the behavior of moisture and optimize industrial processes (Cavalcanti-Mata et al., 2024). Although the use of passion fruit byproducts has increased considerably, information on the combined evaluation of drying kinetics and effects of temperature on the physicochemical and technological properties of peel flour is lacking. In this study, we evaluated drying kinetics and the effect of different temperatures (50, 60, and 70 °C) on the properties of passion fruit peel flour. Our findings may contribute to its sustainable processing and support its industrial application as a value-added ingredient.

## Material and Methods

In order to obtain the peel, passion fruits were collected from the field of the IF Goiano experimental farm, Rio Verde Campus (17º 48’ 24” S; 50º 53’ 57” W). Mature passion fruit of the species *Passiflora edulis* Sims., cultivar UENF Rio Dourado, a cultivar capable of producing about 25 tons per hectare (Viana et al., 2016), were harvested about 70–80 days after blossoming. After harvesting, the fruits were transported to the Laboratory of Post-harvest of Vegetable Products (LPCPV), where the seeds were removed, and the peel was separated from the pulp. The peels were placed in a BOD chamber at 5 °C for 24 h to make the moisture content uniform. Before drying, the initial moisture content was determined by three samples of 15 g for 24 h in a forced-air circulation oven at 105 ±1 °C.

After determining the moisture content, the passion fruit peels were dried at 50, 60, and 70 °C and relative humidity of 14.35, 7.78, and 6.25%, respectively, using fully perforated trays; each tray contained 152.49 ±1.6 g of product. The peels were cut lengthwise, obtaining four to six pieces of cut peel from each fruit, depending on the fruit size, to obtain portions of similar sizes with a length of 9.11 ±0.2 cm, a width of 5.73 ±0.2 cm, and a thickness of 0.79 ±0.1 cm. Drying was monitored by mass loss; the trays were periodically weighed at initial intervals of 10 min on a semi-analytical scale with a resolution of 0.01 g. The drying process was monitored until the samples reached a constant mass, corresponding to the equilibrium moisture content under each condition.

### Mathematical modeling

Based on the experimental data, the initial moisture content, equilibrium moisture content, and moisture content throughout the drying process, we calculated the moisture content ratio values using Equation 1.

$$MR = \frac{MC - EMC}{MC_i - EMC} \tag{1}$$

where MR is the moisture content ratio (dimensionless), MC is the product moisture content (decimal, db), EMC is the equilibrium moisture content (decimal, db), and $MC_i$ is the initial moisture content (decimal, db).

Using experimental data on MR and time, mathematical models (Equations 2, 3, 4, 5, 6, 7, 8, 9, 10, 11, and 12) were adjusted for the drying of passion fruit peel, using models commonly implemented to represent the drying of agricultural products (Table 1).

**Table 1**: Mathematical models used to predict the drying kinetics of agricultural products (Siqueira et al., 2020; Reis et al., 2023).

| Model designation | Model | Equation |
|---|---|---|
| Page | $MR = \exp(-k\ t^n)$ | (02) |
| Midilli | $MR = a \exp(-k\ t^n) + b\ t$ | (03) |
| Newton | $MR = \exp(-k\ t)$ | (04) |
| Thompson | $MR = \exp\{[-a - (a^2 + 4\ b\ t)^{0.5}] / (2\ b)\}$ | (05) |
| Henderson and Pabis | $MR = a \exp(-k\ t)$ | (06) |
| Verna | $MR = - a \exp(-k\ t) + (1 - a) \exp(-k_1\ t)$ | (07) |
| Logarithmic | $MR = a \exp(-k\ t)$ | (08) |
| Two-term exponential | $MR = a \exp(-k\ t) + (1 - a) \exp(-k\ a\ t)$ | (09) |
| Two terms | $MR = a \exp(-k_0\ t) + b \exp(-k_1\ t)$ | (10) |
| Approximation of diffusion | $MR = a \exp(-k\ t) + (1-a) \exp(-k\ b\ t)$ | (11) |
| Valcam | $MR = a + b + c\ t^{1.5}\ d\ t^2$ | (12) |

where t is the drying time; k, $k_0$, $k_1$ are the drying constants; a, b, c are the model coefficients.

The effective diffusion coefficient was determined by adjusting the mathematical model of liquid diffusion (Equation 13) to the experimental data on the drying of passion fruit peel, based on the geometric form of an infinite flat plate with an approximation of eight terms (Silva et al., 2015) and the boundary condition of known moisture content on the surface of the product (Brooker, Bakker-Arkema & Hall, 1992).

$$MR = \frac{MC - EMC}{MC_i - EMC} = \frac{8}{\pi^2} \sum_{n=1}^{\infty} \frac{1}{(2n+1)^2} \exp - \left[ \frac{(2n+1)^2 \pi^2 D_{ef}}{9} \left( \frac{t}{4r} \right)^2 \right] \quad (13)$$

where $D_{ef}$ is the liquid diffusion coefficient ($m^2\ s^{-1}$), t is the drying time (h), r is the product thickness (m); and n is the number of terms in the model.

The thickness was determined using a digital caliper that had a resolution of 0.01 mm, using 50 pieces of passion fruit, measured at three points on each side.

We evaluated the effect of temperature on the drying process in relation to the effective diffusion coefficient using the Arrhenius equation (Equation 14). By applying the natural logarithm in Equation 14, from the relationship Ln ($D_{ef}$) as a function of the inverse of temperature ($T^{-1}$), a straight line (Equation 15) was obtained to estimate the activation energy as the slope of the linear regression line.

$$D_{ef} = D_0 \exp\left( \frac{-E_a}{RT} \right) \quad (14)$$

$$LnD_{ef} = LnD_0 - \left( \frac{E_a}{R} \right) \frac{1}{T} \quad (15)$$

where $D_0$ represents the pre-exponential factor ($m^2\ s^{-1}$), $E_a$ is the activation energy ($kJ\ mol^{-1}$), R is the universal gas constant (8.314 $kJ\ kmol^{-1}\ K^{-1}$), and T stands for the drying air temperature (K).

The experimental data on the drying of passion fruit peel were subjected to mathematical drying kinetics model fitting using nonlinear regression analysis by the Gauss-Newton method, considering the magnitude of the adjusted coefficient of determination ($R^2$), the relative mean error (RME), and the estimated mean error (SE) as criteria for defining the quality of the fit (Equations 16 and 17).

$$RME = \frac{100}{n} \sum_{i=1}^{n} \left( \frac{\left| Y - \hat{Y} \right|}{Y} \right) \quad (16)$$

$$SE = \sqrt{\frac{\sum_{i=1}^{n} \left( Y - \hat{Y} \right)^2}{DF}} \quad (17)$$

where Y is the experimentally observed value, $\hat{Y}$ is the value estimated by the model, n is the number of experimental observations, and DF is the degrees of freedom of the model (difference between the number of observations and the number of model parameters).

The models preselected by the Gauss-Newton criterion were submitted to the Akaike Information Criterion (AIC) and the Schwarz Bayesian Information Criterion (BIC) (Equations 18 and 19) as complementary criteria for model selection, due to their high accuracy.

$$AIC = -2 \log \ell + 2p \quad (18)$$

$$BIC = -2 \log \ell + pLn(n) \quad (19)$$

where p and n is the number of parameters and observations in the model; $\ell$ is the maximum likelihood, considering the parameter estimates.

### Technological properties of passion fruit peel flour

The dried passion fruit peels were ground using a Willye mill (Tecnal, R-TE-650/1) to a granularity of 10 mesh, then packed in low-density polyethylene bags and stored in a refrigerated environment at 18 °C. The treatments were denoted as F50, F60, and F70, corresponding to passion fruit peel flour dried at 50, 60, and 70 °C, respectively.

To determine water absorption capacity (WAC), 0.5 g of passion fruit peel flour (PFPF) was added to 25 mL of water in Falcon tubes, shaken for 1 min, and centrifuged at 5,300 rpm for 20 min. The supernatant was collected and used to determine water solubility (WS, Equation 20), and WAC was calculated using Equation 21. The supernatant was placed in a Petri dish and dried to constant weight, and WS was calculated using Equation 20.

$$Water\ solubility\left(WS\right)=\frac{Evaporation\ residue\left(g\right)}{Sample\ mass\left(g,\mathrm{db}\right)} \tag{20}$$

$$Water\ absorption\ capacity\left(WAC\right)=\frac{Water\ absorbed\ by\ the\ sample\left(g\right)}{Sample\ mass\left(g,\mathrm{db}\right)} \tag{21}$$

The emulsifying activity was determined by weighing 1 g of sample, 10 mL of water, and 10 mL of soybean oil, and the mixture was stirred and distributed into 15 mL graduated Falcon tubes. After that, the contents were centrifuged at 3,000 xg for 5 min, and the emulsifying activity was calculated using Equation 22 (Ogunwolu et al., 2009).

$$Emulsifying\ activity\left(EA\right)=\frac{Emulsifying\ layer\left(mL\right)}{Total\ volume\ in\ the\ tube\left(mL\right)} \tag{22}$$

The color of the sample was determined using a Color Flex EZ spectrophotometer, with nine repetitions for each sample. The L, a*, and b* coordinates were read directly and subsequently converted to Chroma (C*, Equation 23) and hue angle (H*, Equation 24) (Demirhan & Özbek, 2009).

$$C^*=\sqrt{\left(a^*\right)^2+\left(b^*\right)^2} \tag{23}$$

$$H^*=tan^{-1}\left(\frac{b^*}{a^*}\right) \tag{24}$$

### Physicochemical characterization of PFPF

The fixed mineral residue (ash) content was determined by incinerating 3 g of flour placed in porcelain containers until light-colored ash was obtained in a muffle furnace at 550 °C, following the method described by (Association of Official Analytical Chemists- AOAC, 1995), and Equation 25 was used for the calculation.

$$\mathrm{Ash}\left(\mathrm{g100g^{-1}}\right)=\frac{\text{Final sample mass}\left(\mathrm{g}\right)}{\text{Initial sample mass}\left(\mathrm{g,db}\right)}\times 100 \tag{25}$$

Lipids were extracted using the Soxhlet method (AOAC, 1995). Briefly, 3 g of flour was added to the filter paper. The extractor was attached to a flat-bottom flask with a known mass and dried at 105 °C, with enough hexane added for one and a half Soxhlet extractions (about 400 mL of hexane). By heating the flask on an electric hotplate, extraction was continued for 8 h. The tied filter paper was removed, the distillate containing hexane and the extracted residue were coupled in a rotary evaporator for separation, and then the contents were weighed. The percentage of lipids was calculated using Equation 26.

$$\mathrm{Lipids}\left(\mathrm{g100g^{-1}}\right)=\frac{\mathrm{N}}{\mathrm{P}}\times 100 \tag{26}$$

where N is the lipid mass (g), and P is the total sample mass (g, db).

The pH was determined using a PHS-3E digital bench potentiometer, with 3 g of PFPF diluted in 150 mL of distilled water. Briefly, the electrode was inserted into the beaker containing the sample, and the pH was measured at different points to obtain a more accurate reading, following the methodology provided by the Adolfo Lutz Institute (Instituto Adolfo Lutz - IAL, 2008).

Total titratable acidity was determined by titration with a standardized base, using a potentiometer, until the pH of solution reached about 8.2. A 0.1 N sodium hydroxide solution was used as the titrant, and 1% phenolphthalein was used as the indicator (IAL, 2008). Titratable acidity was calculated using Equation 27.

$$\text{Titratable acidity }\left(\mathrm{TA}\right)=\frac{\mathrm{V}\times\ \mathrm{f}\times 100}{\mathrm{P}} \tag{27}$$

where V is the volume of sodium hydroxide solution used in titration (mL); f is the correction factor for sodium hydroxide solution; and P is the amount of sample used in titration (g or mL).

### Antioxidant capacity

The extract was prepared following the methodology described by Larrauri, Rupérez and Saura-Calixto (1997) with modifications. Briefly, 2 g of PFPF was added to 40 mL of 50% methanol, homogenized, and filtered after 60 min. The supernatant was transferred to a flask (100 mL). To the residue from the first extraction, 40 mL of 70% acetone was added. After 60 min, the supernatant was transferred to the flask containing the first supernatant, and the volume was made up to 100 mL with distilled water.

The scavenging of the DPPH• radical (2,2-diphenyl-1-picrylhydrazyl) was determined following the method proposed by Brand-Williams, Cuvelier and Berset (1995), with modifications. Aliquots of 0.1 mL of the extracts were added to 3.9 mL of DPPH methanolic solution (25 mg $L^{-1}$) and kept at room temperature for 30 min under controlled illumination. The absorbance of the samples was determined at 515 nm using a UV/Visible spectrophotometer (UV-5100 Spectrophotometer, Metash), and the percentage of discoloration was calculated using Equation 28.

$$\%\ \text{Descoloration} = \left[1 - \frac{\text{Sample absorbance}}{\text{Absorbance control}}\right] \times 100 \quad (28)$$

## Scanning electron microscopy (SEM)

The images were obtained using a Jeol JSM7100F field emission scanning electron microscope (FEG-SEM) with an electron acceleration voltage of 5 keV in the secondary electron detection (SED) mode.

## Statistical analysis

The experiment was conducted using a completely randomized design at three drying air temperatures (50, 60, and 70 °C) and with five replicates. The results obtained from the analyses of technological and physicochemical properties were evaluated by analysis of variance and multiple comparisons using the Scott-Knott test. All results were considered to be statistically significant at $p < 0.05$.

# Results and Discussion

## Modeling of the drying process of passion fruit peel

The passion fruit peel was dried with an initial moisture content of 86.93 ±0.36% on a wet basis (wb) until it reached a final moisture content of 8.96 ±0.19% wb. To reach the final moisture content, 30.5, 17.0, and 9.5 h were required for drying air temperatures of 50, 60, and 70 °C, respectively. Equilibrium moisture contents were achieved with moisture contents of 8.36 ±0.02, 5.16 ±0.33, and 4.22 ±0.27% at 50, 60, and 70 °C, respectively. As the drying air temperature increased, drying time decreased as the rate of water removal from the product was higher, especially in the initial stage of the drying process, which decreased over time (Figure 1).

The behavior of moisture content curves is consistent with the temperatures applied in this study, as the evaporative capacity of air increases with rising temperatures. Additionally, at higher temperatures, the relative humidity of the drying air is lower, which increases the partial water vapor pressure gradient, as reported in several studies on the drying kinetics of various agricultural products (Bezerra et al., 2015; Martins et al., 2019; Siqueira et al., 2020; Wanderley et al., 2023).

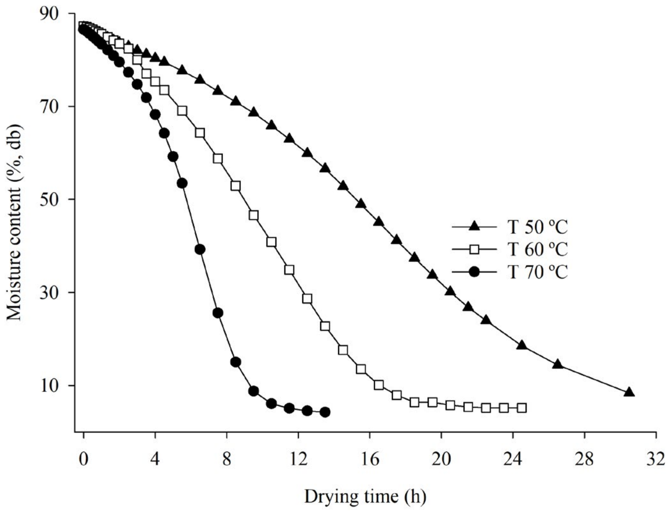


**Figure 1**: Moisture content of passion fruit peels during drying at 50, 60, and 70 °C.

The values for the evaluation of the various drying kinetics models for passion fruit peel are presented in Table 2. This method considers three parameters for evaluation, including coefficient of determination ($R^2$), relative mean error (RME), and standard error (SE). RME is an exclusionary parameter, and only those models with RME values below 10% are considered valid (Mohapatra & Rao, 2005). In this context, none of the models showed adequate adjustment for all temperatures tested. However, some models were satisfactory for specific drying air conditions, notably the Page (02) model for drying at 60 °C, Midilli (03) for drying at 50 and 60 °C, and Valcam (12) for drying at 50 and 70 °C. The other models did not fit any of the conditions studied.

The $R^2$ and SE were also considered for validation of the previously selected models based on the RME values. The models presenting lower SE values and $R^2$ values greater than 0.95 were considered more appropriate; the closer the value of $R^2$ was to 1.0, the better the fit. Under these conditions, among the previously selected models at 50 °C, the Valcam model (12) had the lowest SE, and the $R^2$ values did not differ from those obtained in the Page model (02). At 60 °C, the Page (02) model performed better than Midilli's (03) model in terms of SE value, although the magnitude was lower than that observed at 50 °C. At 70 °C, the Valcam model (12) also had a lower SE value, and the $R^2$ value was 0.999 for both models.

To reinforce or complement the selection of models, we adopted the parameters AIC and BIC. The AIC and BIC criteria allow researchers to select the best model among those pre-selected by other criteria. The model with the highest absolute values of AIC and BIC is considered to be the best, and this method has been used satisfactorily to complement the selection of drying kinetics models in several studies (Quequeto et al., 2019; Siqueira et al., 2020). Based on these criteria, among the four models pre-selected at the three temperatures, the Page

(02) models at 60 °C and the Valcam (12) models at 50 and 70 °C were the best (Table 2).

The curves that best fit the drying kinetics of passion fruit peels are shown in Figure 2, which include those for Page (02) at 60 °C and Valcam (12) at 50 and 70 °C. The selected models presented an adequate fit; they described the process in relation to the drying behavior of passion fruit peels with satisfactory accuracy. Thus, these models established an adequate correspondence between the observed values and the estimated values. The selected models showed a satisfactory fit when describing the drying of agricultural products with different characteristics and temperature ranges (Quequeto et al., 2019; Silva et al., 2017; Silva et al., 2022). A similar result using the Page model (02) was also obtained in previous studies for passion fruit peel at a temperature range of 45–65 °C (Sittipa et al., 2020).

**Table 2**: The mean errors (SE), relative mean errors (RME), coefficients of determination ($R^2$), Akaike Information Criterion (AIC), and Schwarz's Bayesian Information Criterion (BIC) for passion fruit peel drying kinetics at 50, 60, and 70 °C.

| Model | Temperature (°C) | SE | RME (%) | $R^2$ | AIC | BIC |
|---|---|---|---|---|---|---|
| Page | 50 | 0.015 | 72.330 | 0.998 | | |
| | 60 | 0.012 | 9.498 | 0.999 | -162.097 | -158.100 |
| | 70 | 0.022 | 33.358 | 0.996 | | |
| Midilli | 50 | 0.008 | 4.947 | 0.999 | -249.156 | -241.102 |
| | 60 | 0.013 | 8.607 | 0.999 | -158.188 | -151.527 |
| | 70 | 0.011 | 17.006 | 0.999 | | |
| Newton | 50 | 0.015 | 78.435 | 0.998 | | |
| | 60 | 0.036 | 53.226 | 0.991 | | |
| | 70 | 0.037 | 64.372 | 0.988 | | |
| Thompson | 50 | 0.015 | 78.463 | 0.998 | | |
| | 60 | 0.036 | 53.243 | 0.991 | | |
| | 70 | 0.038 | 64.377 | 0.988 | | |
| Henderson and Pabis | 50 | 0.015 | 82.393 | 0.998 | | |
| | 60 | 0.027 | 39.943 | 0.995 | | |
| | 70 | 0.034 | 57.597 | 0.991 | | |
| Verna | 50 | 0.065 | 38.796 | 0.967 | | |
| | 60 | 0.025 | 24.944 | 0.996 | | |
| | 70 | 0.301 | 32.652 | 0.288 | | |
| Logarithmic | 50 | 0.008 | 28.288 | 0.999 | | |
| | 60 | 0.021 | 18.779 | 0.997 | | |
| | 70 | 0.012 | 21.474 | 0.999 | | |
| Two-term Exponential | 50 | 0.014 | 80.451 | 0.998 | | |
| | 60 | 0.036 | 53.227 | 0.991 | | |
| | 70 | 0.037 | 64.373 | 0.988 | | |
| Two terms | 50 | 0.015 | 80.165 | 0.998 | | |
| | 60 | 0.012 | 15.874 | 0.999 | | |
| | 70 | 0.036 | 57.599 | 0.991 | | |
| Approximation of diffusion | 50 | 0.010 | 28.294 | 0.999 | | |
| | 60 | 0.024 | 24.944 | 0.996 | | |
| | 70 | 0.010 | 19.294 | 0.999 | | |
| Valcam | 50 | 0.004 | 6.615 | 0.999 | -295.945 | -287.891 |
| | 60 | 0.021 | 19.274 | 0.997 | | |
| | 70 | 0.005 | 4.245 | 0.999 | -154.684 | -149.462 |

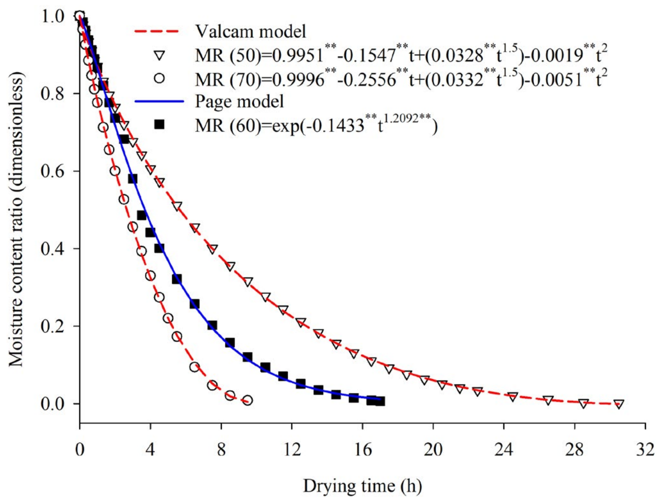


**Figure 2**: The change in the moisture content ratio of passion fruit peels according to the Page (60 °C) and Valcam (50 and 70 °C) models.

** Significant at p<0.01 by t-test.

## Effective diffusion coefficient of the dried passion fruit peel

The effective diffusion coefficient values and the Arrhenius representation for the drying process of passion fruit peels in the temperature range of 50–70 °C, obtained by adjusting the experimental values using the eight-term mathematical model of liquid diffusion for a flat form, are shown in Figures 3A-B.

The effective diffusion coefficient varied between $6.87213 \times 10^{-10}$ and $15.0443 \times 10^{-10}$ $m^2\ s^{-1}$ for a temperature range of 50–70 °C, with an adjustment level of 99.68%, which explained the level of variation in the effective diffusion coefficient in relation to temperature. The increase in the drying air temperature was proportional to the increase in the effective diffusion coefficient, which indicated an interdependence between the amount of water removed and the magnitude of the temperature.

As the drying air temperature decreased, the level of internal resistance to water transport during drying increased, which resulted in lower values for the effective diffusion coefficient. This behavior can be explained by the reduction in the magnitude of water diffusion from the center to the periphery, especially when the moisture content is lower, which is associated with more strongly bound water molecules (Lima et al., 2016). The increase in the effective diffusion coefficient with an increase in the drying temperature observed in this study is consistent with the findings of recent studies, which reported that temperature is a key factor governing the migration of internal moisture during the drying process. For example, studies on the drying of fruits and vegetables have shown that effective moisture diffusivity increases significantly with temperature due to an increase in molecular mobility and a decrease in internal resistance to water transport (Nguyen & Nguyen, 2025).

Similarly, in agro-industrial residues, such as pineapple peel and similar plant-based materials, higher drying temperatures were associated with accelerated mass transfer and higher diffusivity values, which indicated that diffusion mechanisms greatly depend on thermal conditions (Cavalcanti-Mata et al., 2024; Reis et al., 2023). These findings support the patterns observed for passion fruit peel, where higher temperatures (50–70 °C) promoted greater removal of moisture and increased effective diffusion coefficients, reflecting an improvement in internal water mobility and reduction in resistance to mass transfer.

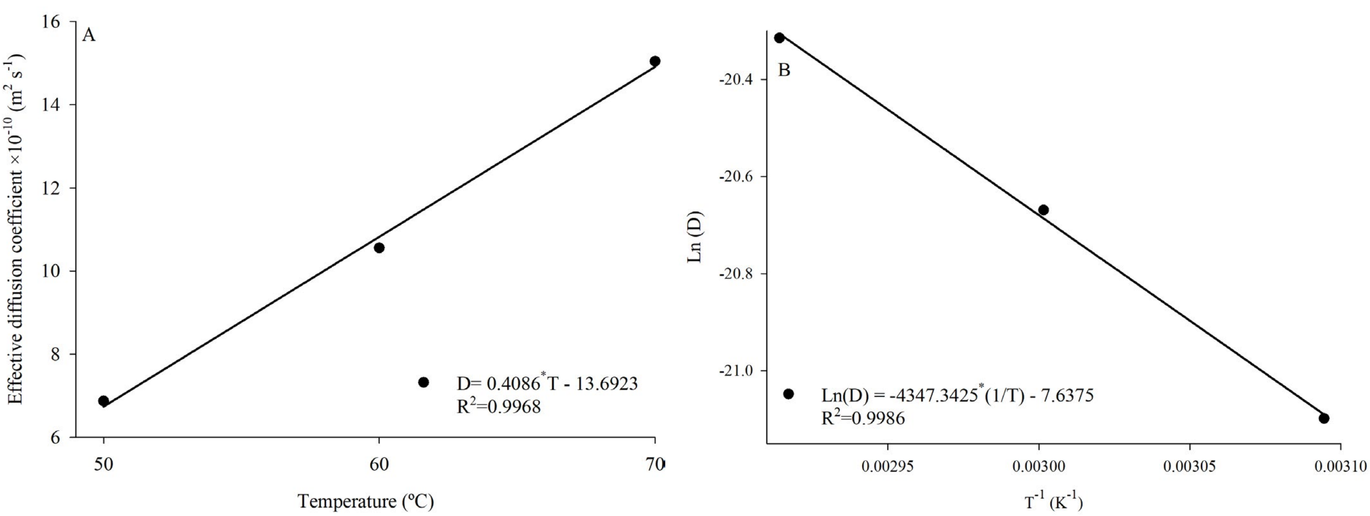


**Figure 3**: Effective diffusion coefficient (A) and Arrhenius representation (B) for drying air temperatures (50, 60, and 70 °C) of passion fruit peel are presented.

* Significant at p<0.05 by t-test.

The minimum energy required to trigger the start of the passion fruit peel drying process was 36.14 kJ mol$^{-1}$, which is within the range of 12.70–110 kJ mol$^{-1}$ reported by Zogzas, Maroulis and Marinos-Kouris (1996) for various vegetable products. The minimum energy required recorded in this study is close to that (34.73 kJ mol$^{-1}$) reported by Bezerra et al. (2015), who studied passion fruit peels within a similar temperature range.

## Effect of different drying temperatures on the quality of dried passion fruit peel

The results obtained by conducting the analysis of variance for the parameters of color, technological properties, physicochemical properties, and antioxidant activity for PFPF are presented in Table 3. The influence of the drying air temperature was observed in most of the variables, except for the WAC, WS, and ash analyses. The coefficients of variance ranged from 0.40 to 45.84%, with only one (WAC) above 30% as established by Pimentel-Gomes (2022).

The mean values obtained experimentally for the parameters of color, emulsifying activity, lipids, pH, titratable acidity, and DPPH for the PFPF obtained at three drying air temperatures (50, 60, and 70 °C) are presented in Table 4. The L parameter ranges from black (0) to white (100), with L values ranging from 81.38 to 74.33, inversely proportional to temperature. Significant differences in the red-green coordinate (a*) were found among F50, F60, and F70 (0.62, 2.84, and 4.13, respectively) ($p < 0.05$). The yellow-blue coordinate F60 (b*) had a value of 25.12, whereas F50 had a value of 23.04, again with significant differences between them ($p < 0.05$). Similarly, significant differences in hue angles were found between F50 and both F60 and F70 (88.47, 83.54, and 79.63, respectively) ($p < 0.05$).

In relation to technological analyses, WAC and WS behaved randomly, i.e., no effect of drying air temperature was observed, and their values were 12.10 g g$^{-1}$ and 27.68 g g$^{-1}$, respectively. WAC is used to determine the amount of water that a fiber can absorb when an excess of water is present. These properties play an important role in baking applications as they directly affect the texture of the product, keeping it moist and soft (Giuntini, Lajolo, & Menezes, 2003).

The lipid content ranged from 0.48 to 0.71, with F50 showing the highest content, indicating that temperature had an effect. This value was relatively close (0.96 g 100g$^{-1}$) to that reported by Guimarães et al. (2023), who studied one cultivar of *Passiflora cincinnata* Mast, aiming to obtain byproducts. The pH was affected by temperature, and the results obtained were 5.16, 4.74, and 4.54, demonstrating a slight but significant range of variation in practical terms. The lowest pH (highest acidity) was recorded in F70.

Although higher drying temperatures (60 and 70 °C) improved mass transfer and decreased drying time, they negatively affected important qualities of the flour. In contrast, the physicochemical properties of the sample dried at 50 °C (F50) were better preserved; these properties included higher luminosity, higher pH, lower acidity, and higher lipid content. This finding indicated that the sample underwent lower thermal degradation.

**Table 3:** Analysis of variance performed for color variables (L, a*, b*, chroma, and hue angle), technological variables (WAC, WS, and EA), physicochemical variables (ash, lipids, pH, and TA), and antioxidant activity (DPPH).

| Variables | DF | MS | F | Mean | CV (%) |
|---|---|---|---|---|---|
| L | 2 | 67.20 | 90.87** | 77.27 | 1.11 |
| a* | 2 | 15.74 | 1593.80** | 2.53 | 3.93 |
| b* | 2 | 9.40 | 7.64** | 23.57 | 4.71 |
| Chroma | 2 | 8.84 | 7.26** | 23.75 | 4.65 |
| Hue angle | 2 | 98.25 | 865.08** | 83.88 | 0.40 |
| WAC | 2 | 1.35 | 0.79$^{ns}$ | 12.10 | 10.83 |
| WS | 2 | 176.89 | 1.09$^{ns}$ | 27.68 | 45.84 |
| EA | 2 | 452.92 | 11.382** | 49.17 | 12.83 |
| Ash | 2 | 1.63 | 1.45$^{ns}$ | 6.66 | 15.97 |
| Lipids | 2 | 0.07 | 4.99* | 0.58 | 20.27 |
| pH | 2 | 0.51 | 1041.66** | 4.81 | 0.46 |
| TA | 2 | 43.16 | 85.29** | 9.49 | 7.49 |
| DPPH | 2 | 24.77 | 3.53* | 16.70 | 15.85 |

Note: DF – Degrees of freedom, MS – Mean square of treatment, F – Value calculated by Fisher's test, WAC – Water absorption capacity, WS – Water solubility; EA – Emulsifying activity, TA – Titratable acidity, DPPH – Percentage of discoloration, CV – Coefficient of variation; ** Significant (p<0.01), * Significant (p<0.05) and $^{ns}$Not significant by the F test.

**Table 4:** Evaluation of color (A), physicochemical properties, and technological properties (B) of PFPF as a function of drying air temperature.

| | Flour | L | a* | b* | Chroma | Hue angle | Graphical color |
|---|---|---|---|---|---|---|---|
| (A) | F50 | 81.38±1.22 a | 0.62±0.10 c | 23.04±0.83 b | 23.05±0.84 b | 88.47±0.20 a | |
| | F60 | 76.11±1.01 b | 2.84±0.20 b | 25.12±1.32 a | 25.28±1.32 a | 83.54±0.47 b | |
| | F70 | 74.33±0.50 c | 4.13±0.08 a | 22.53±0.23 b | 22.91±0.23 b | 79.63±0.19 c | |
| | Flour | EA | Lipids | pH | TA | DPPH | |
| (B) | F50 | 48.5±9.28 b | 0.71±0.09 a | 5.16±0.03 a | 6.28±0.74 c | 16.37±2.37 a | |
| | F60 | 59.00±5.18 a | 0.48±0.15 b | 4.74±0.17 b | 10.15±0.79 b | 15.23±3.61 a | |
| | F70 | 40.00±2.50 b | 0.54±0.11 b | 4.54±0.01 c | 12.04±0.58 a | 18.50±1.56 b | |

Note: *Pairs of equal letters in the column do not differ from each other by the Scott Knott test ($p<0.05$).

The antioxidant capacities of PFPF were measured by DPPH radical scavenging and expressed as a percentage of discoloration. The drying air temperature had a positive effect, with F70 presenting the highest percentage of discoloration (18.50%). This can be explained by the enhanced extractability of phenolic compounds and the formation of antioxidant Maillard reaction products under higher thermal conditions. The higher antioxidant activity observed in F70 suggests that PFPF may serve as a functional ingredient with potential health-promoting properties when incorporated into the human diet (Zujko & Witkowska, 2023).

## Scanning electron microscope images of PFPF after drying

The scanning electron microscope images of PFPF obtained at different drying temperatures (50, 60, and 70 °C) are shown in Figure 4. The images of the flour samples were obtained to verify their morphological structure at different drying temperatures.

The images showed irregular surfaces with smooth and striated parts, and fibers showed elongated characteristics. Proteins and starch could not be identified due to their low content. The flour obtained at 50 °C had a more homogeneous structure and thinner plant tissue walls (Figure 4A) compared to the flour obtained at other temperatures (Figures 4B and 4C). This characteristic is desirable due to the ease with which the product breaks down when chewed, which is a trait desired by consumers (Alves & Ascheri, 2016).

As the drying temperature increased, the plant tissue became more compact (Figures 4B and 4C), which increased tissue thickness. This characteristic is related to sensitivity to drying temperatures above 50 °C.

Drying at 60 °C and 70 °C resulted in faster water removal than drying at 50 °C due to an increase in internal vapor pressure, which increased the movement of water molecules and caused vegetable tissues to rupture. Kazemi et al. (2019) reported that this behavior is related to the disintegration of heat-sensitive compounds and damage caused by temperature, resulting in structural compaction.

Overall, the results of the microstructural analysis revealed that lower temperatures maintained a more homogeneous structure with thinner cell walls, whereas higher temperatures caused tissue compaction and structural damage. Therefore, 50 °C was selected as the optimal drying temperature based on the balance between drying efficiency and preservation of quality, favoring conditions that maintain the structural and functional integrity of the product.

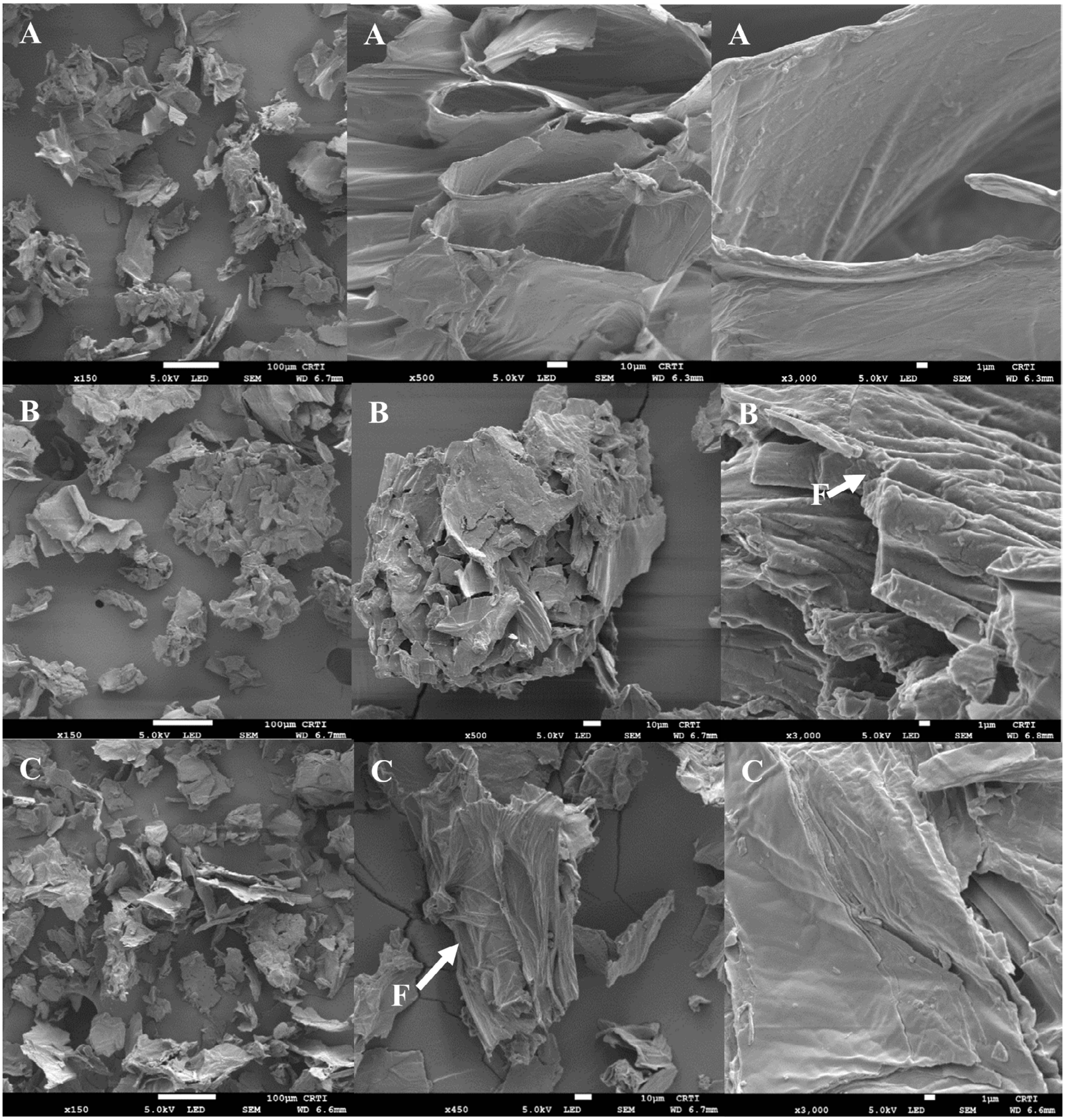


**Figure 4:** Scanning electron microscope images (150X, 100 μm) of PFPF were obtained at drying temperatures of 50 °C (A), 60 °C (B), and 70 °C (C). Note: F- fiber.

## Conclusions

Drying behavior of passion fruit peel was strongly influenced by temperature, confirming its role in heat and mass transfer during drying. The Valcam model best described drying at 50 and 70 °C, while the Page model was more suitable at 60 °C. Effective diffusivity increased with temperature, and activation energy was 36.144 kJ $mol^{-1}$. Drying at 50 °C preserved quality attributes best. PFPF showed potential as a functional ingredient, though further studies on sensory properties and stability are needed.

## Author Contributions

Conceptual idea: Mabasso, G.A.; Almeida, A.B.; Ferreira, S.V.; Célia, J.A.; Resende, O.; Oliveira, D.E.C.; Methodology design: Mabasso, G.A.; Almeida, A.B.; Ferreira, S.V.; Célia, J.A.; Data collection: Mabasso, G.A.; Almeida, A.B.; Ferreira, S.V.; Célia, J.A.; Data analysis and interpretation: Mabasso, G.A.; Almeida, A.B.; Ferreira, S.V.; Célia, J.A.; Resende, O.; Oliveira, D.E.C., and Writing and editing: Mabasso, G.A.; Almeida, A.B.; Ferreira, S.V.; Célia, J.A.; Resende, O.; Oliveira, D.E.C.

## Acknowledgements

PIAT IF Goiano, CAPES, FAPEG, FINEP, and CNPq for the financial support essential to the execution of this work.

## Data Availability Statement

Data available upon request to authors.

## References

Alves, P. L. da S., & Ascheri, J. L. R. (2016). Analise por imagem e microscopia electrônica por varredura das farinhas extrudadas de arroz e maracujá. *Higiene Alimentar*, *30*:144-148.

Association of Official Analytical Chemists - AOAC. (1990). *Official analytical chemists*. (14th Edition), Washington, 1094p.

Betancur-Ancona, D. et al. (2025). Functional, bioactive, and sensory properties of nutraceutical beverages enriched with passion fruit (*Passiflora edulis*) peel fiber. *Food Chemistry Advances*, *7*:101005.

Bezerra, C. V. et al. (2015). A modeling study for moisture diffusivities and moisture transfer coefficients in drying of passion fruit peel. *International Journal of Heat and Mass Transfer*, *85*:750-755.

Brand-Williams, W., Cuvelier, M. E., & Berset, C. L. W. T. (1995). Use of a free radical method to evaluate antioxidant activity. *LWT-Food Science and Technology*, *28*(1):25-30.

Brooker, D. B., Bakker-Arkema, F. W., & Hall, C. W. (1992). *Drying and storage of grains and oilseeds*. Springer Science & Business Media. 450p.

Cavalcanti-Mata, M. E. R. et al. (2024). Residue from passion fruit processing industry: Application of mathematical drying models for seeds. *Processes*, *12*(8):1752.

Demircan, B., Velioglu, Y. S., & Giuffrè, A. M. (2023). Bergamot juice powder with high bioactive properties: Spray-drying for the preservation of antioxidant activity and ultrasound-assisted extraction for enhanced phenolic compound extraction. *Journal of Food Science*, *88*(9):3694-3713.

Demirhan, E., & Özbek, B. (2009). Color change kinetics of microwave-dried basil. *Drying Technology*, *27*(1):156-166.

Fonseca, A. M., Silvestre, A. J., & Rocha, S. M. (2025). From physicochemical characteristics variability to purple passion fruit (*Passiflora edulis* f. *edulis*) powders nutritional value: On the path of zero-waste. *Journal of the Science of Food and Agriculture*, *105*(6):3306-3316.

Giuntini, E. B., Lajolo, F. M., & de Menezes, E. W. (2003). Potencial de fibra alimentar em países ibero-americanos: Alimentos, produtos e resíduos. *Archivos Latinoamericanos de Nutrición, 53*(1):14-20.

Guimarães, M. L. L. et al. (2023). Coprodutos agroindustriais de maracujá do mato (*Passiflora cincinnata* Mast): qualidade nutricional e funcional. *Research, Society and Development*, *12*(8):e4212842788.

Gunjal, M. et al. (2025). Effect of convective drying temperature and tray load density on bioactive compounds, antioxidant properties, and functional quality of radish Sango microgreens. *Food Chemistry*, *488*:144810.

Instituto Adolfo Lutz -IAL (2008). *Métodos físico-químicos para análise de alimentos*. São Paulo: Instituto Adolfo Lutz, 1020p.

Infante-Neta, A. A. et al. (2026). waste valorization of passion fruit peel hydrolysate for bacterial cellulose production: Influence of nitrogen source on yield and functional properties for food packaging. *Foods*, *15*(5):888.

Junghans, T. G. (2022). *Espécies de maracujazeiro: Uma riqueza do Brasil*. Cruz das Almas, BA: Embrapa Mandioca e Fruticultura, 203p.

Kaur, S. et al. (2023). Utilisation of *Kinnow* peel as a functional ingredient in bread: Physicochemical, functional, textural and sensory attributes. *International Journal of Food Science and Technology*, *58*(5):2706-2714.

Kazemi, M. et al. (2019). Pistachio green hull pectin: Optimization of microwave-assisted extraction and evaluation of its physicochemical, structural and functional properties. *Food Chemistry*, *271*:663-672.

Larrauri, J. A., Rupérez, P., & Saura-Calixto, F. (1997). Effect of drying temperature on the stability of polyphenols and antioxidant activity of red grape pomace peels. *Journal of Agricultural and Food Chemistry*, *45*(4):1390-1393.

Leão, K. M. et al. (2014). Odor potency, aroma profile and volatiles composition of cold pressed oil from industrial passion fruit residues. *Industrial Crops and Products*, *58:*280-286.

Lima, A. G. B. et al. (2016). Drying of bioproducts: Quality and energy aspects. In J. Delgado., & A. B. de. Lima. (eds.) *Drying and energy technologies*. Springer International Publishing, v.63, (pp.1-18).

Martínez, R. et al. (2012). Chemical, technological and *in vitro* antioxidant properties of mango, guava, pineapple and passion fruit dietary fiber concentrate. *Food chemistry*, *135*(3):1520-1526.

Martins, M. P. et al. (2019). Stabilization of apple peel by drying. Influence of temperature and ultrasound application on drying kinetics and product quality. *Drying Technology*, *37*(5):559-568.

Mohapatra, D., & Rao, P. S. (2005). A thin layer drying model of parboiled wheat. *Journal of Food Engineering*, *66*(4):513-518.

Moin, A. et al. (2024). Consumer acceptance and sensory properties of wheat-millet composite biscuits fortified with *Moringa oleifera* and *Camellia sinensis* leaves powder. *Current Research in Nutrition and Food Science Journal*, *12*(2):686-698.

Nascimento, E. M. do. et al. (2016). Effects of high-intensity ultrasound on drying kinetics and antioxidant properties of passion fruit peel. *Journal of Food Engineering*, *170*:108-118.

Nguyen, N. M. P. et al. (2019). *In vitro* antioxidant activity and phenolic profiles of tropical fruit by-products. *International Journal of Food Science and Technology*, *54*(4):1169-1178.

Nguyen, T. H., & Nguyen, D. Q. (2025). Effect of moisture content, temperature, and absolute expansion ratio on the effective moisture diffusivity of swell-dried carrots and apples. *Discover Food*, *5*:412.

Ogunwolu, S. O. et al. (2009). Functional properties of protein concentrates and isolates produced from cashew (*Anacardium occidentale* L.) nut. *Food chemistry*, *115*(3):852-858.

Pimentel-Gomes, F. (2022). *Curso de estatística experimental*. Piracicaba: FEALQ. 451p.

Quequeto, W. D. et al. (2019). Mathematical modeling of thin-layer drying kinetics of *Piper aduncum* L. leaves. *Journal of Agricultural Science*, *11*(8):225-235.

Reis, C. G. D. et al. (2023). Pineapple peel flours: Drying kinetics, thermodynamic properties, and physicochemical characterization. *Processes*, *11*(11):3161.

Santos, L. C. dos et al. (2021). Integrated supercritical $CO_2$ extraction and fractionation of passion fruit (*Passiflora edulis* Sims) by-products. *The Journal of Supercritical Fluids*, *168*:105093.

Silva, F. P. D. et al. (2017). Thermodynamic properties and drying kinetics of *Bauhinia forficata* Link leaves. *Revista Brasileira de Engenharia Agrícola e Ambiental*, *21*(1):61-67.

Silva, L. A. da et al. (2022). Drying effects on Camu-camu residue: An approach of mathematical modeling, thermodynamic properties, and color evaluation in order to obtain a natural food dye. *Journal of Food Processing and Preservation*, *46*(7):e16599.

Silva, L. A. et al. (2015). Cinética de secagem e difusividade efetiva em folhas de jenipapo (*Genipa americana* L.). *Revista Brasileira de Plantas Medicinais*, *17*(4):953-963.

Siqueira, V. C. et al. (2020). Drying kinetics and effective diffusion of buckwheat grains. *Ciência e Agrotecnologia*, *44*:e011320.

Sittipa, C. et al. (2020). Drying kinetics of passion fruit peel for tea products. In *E3S Web of Conferences*. *EDP Sciences*, *187*:04007.

Sousa, E. P. D. et al. (2024). Empirical modeling of the drying kinetics of red beetroot (*Beta vulgaris* L.; Chenopodiaceae) with peel, and flour stability in laminated and plastic flexible packaging. *Foods*, *13*(17):2784.

Teles, G. H. et al. (2023). Full utilization of the yellow passion fruit peel: Chemical characterization and valorization to reduce biomass waste. *Industrial Crops and Products*, *206*:117593.

Viana, A. P. et al. (2016). UENF Rio Dourado: a new passion fruit cultivar with high yield potential. *Crop Breeding and Applied Biotechnology*, *16*(3):250-253.

Wanderley, R. D. O. S. et al. (2023). The temperature influence on drying kinetics and physico-chemical properties of pomegranate peels and seeds. *Foods*, *12*(2):286.

Zogzas, N. P., Maroulis, Z. B., & Marinos-Kouris, D. (1996). Moisture diffusivity data compilation in foodstuffs. *Drying technology*, *14*(10):2225-2253.

Zujko, M. E., & Witkowska, A. M. (2023). Dietary antioxidants and chronic diseases. *Antioxidants*, *12*(2):36.